Supplementary Information

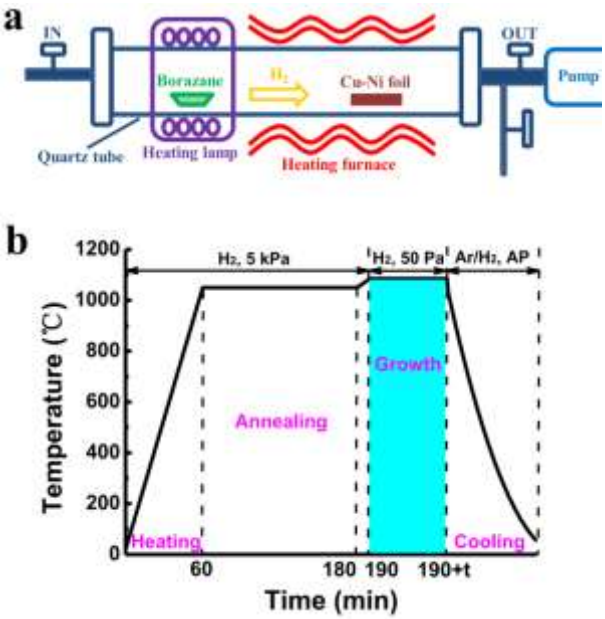

Supplementary Figure 1 | LPCVD setup for h-BN growth and the experimental parameters. (**a**) Schematic diagram of the LPCVD setup for h-BN synthesis. (**b**) Time dependence of experimental parameters for growing h-BN grains.

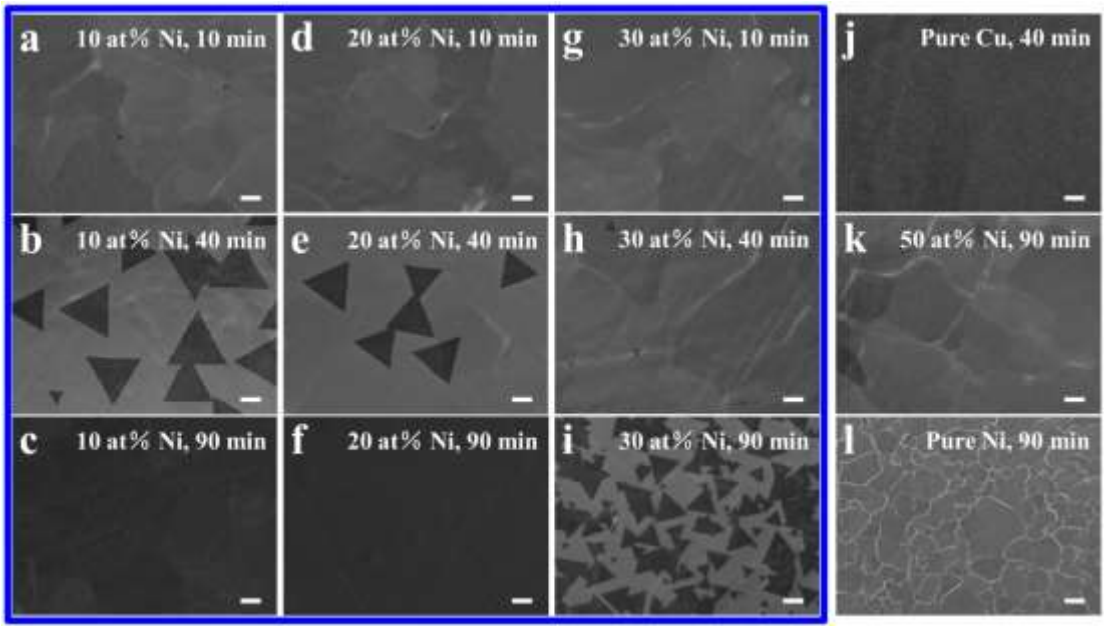

Supplementary Figure 2 | Typical SEM images showing the growth of h-BN at 1,050 °C for different alloy concentrations and growth time. (**a-i**) h-BN grains and films grown on Cu-Ni alloy foils with (**a-c**) 10 atom %, (**d-f**) 20 atom % and (**g-i**) 30 atom % Ni for (**a,d,g**) 10 min, (**b,e,h**) 40 min and (**c,f,i**) 90 min, respectively. (**j**) h-BN film grown on a pure Cu foil for 40 min. (**k-l**) After 90 min of growth, no obvious h-BN grain is observed on both a (**k**) Cu-Ni alloy foil with 50 atom % Ni and a (**l**) pure Ni foil, respectively. The scale bars are 20 μm in all figures.

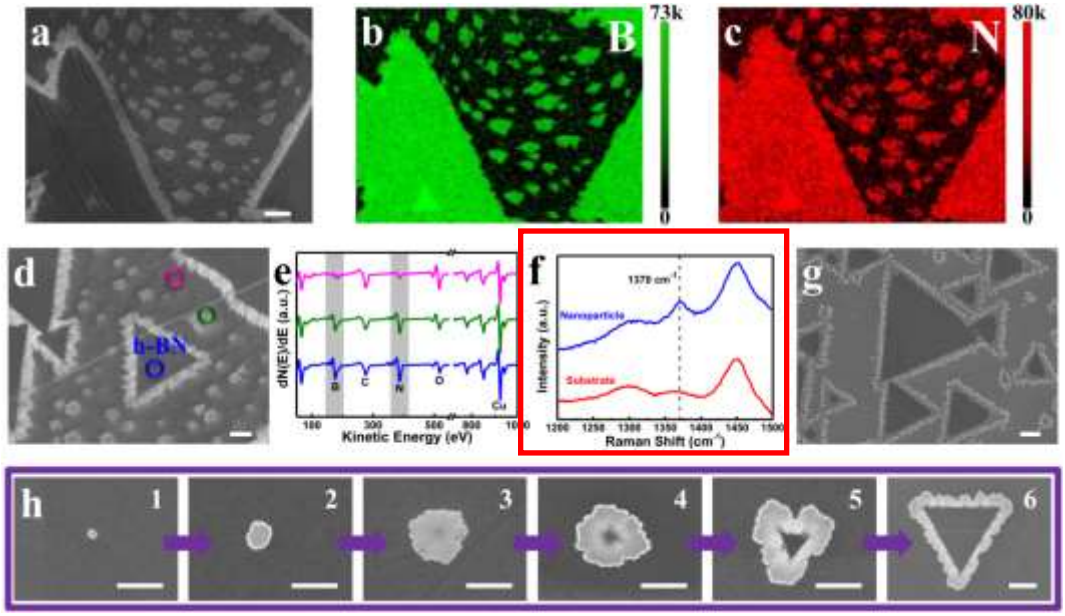

Supplementary Figure 3 | Characterization of the nanoparticles along with h-BN grains. (**a,d**) SEM images of h-BN grains and nanoparticles on Cu foils. (**b-c**) The corresponding B(KLL) and N(KLL) Auger electron maps of (**a**), respectively. (**e**) AES spectra taken in the circled areas in (**d**). It can be seen that besides h-BN grains (blue circle), the nanoparticles (olive circle) also contain a relatively high amount of boron and nitrogen elements. (**f**) Raman spectra taken from nanoparticles transferred on SiO_2/Si as well as from the SiO_2/Si substrate. (**g**) If precursor supply was stopped for a while (5-10 min) at the end of the growth, we can see that h-BN was etched back, separate from the nanoparticles arranged in triangle shape. This indicates that the particles are formed during high temperature growth and not due to the absorption during cooling. (**h**) Images showing the typical evolution of the nanoparticles and the nucleation and growth of h-BN from the particles. All the scale bars are 2μm.

1.方形模型俯视图，矩形模型侧视图。
2.但是怎么知道B和N原子分别在合金的什么位置呢？

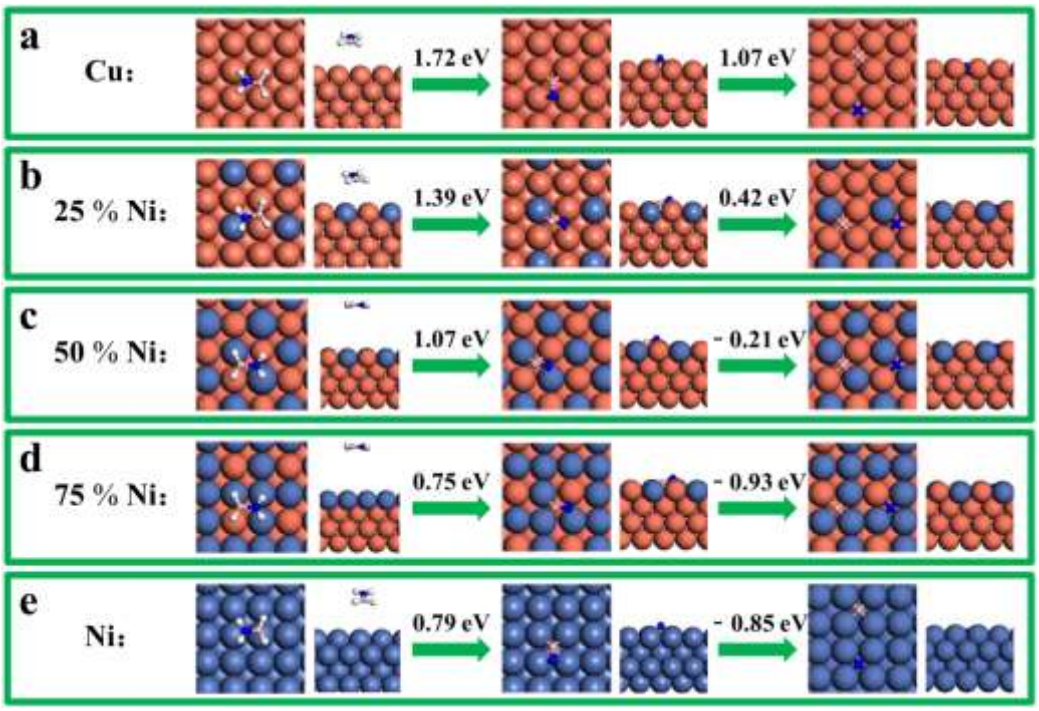

Supplementary Figure 4 | Structures and formation energies of H_2BNH_2 dissociation and BN decomposition on the surfaces of different substrates. The formation energies of different states on (**a**) Cu, (**b**) Cu-Ni alloy with 25 atom % Ni, (**c**) Cu-Ni alloy with 50 atom % Ni, (**d**) Cu-Ni alloy with 75 atom % Ni and (**e**) Ni surface are calculated according to the method presented in the DFT calculation part in the main text.

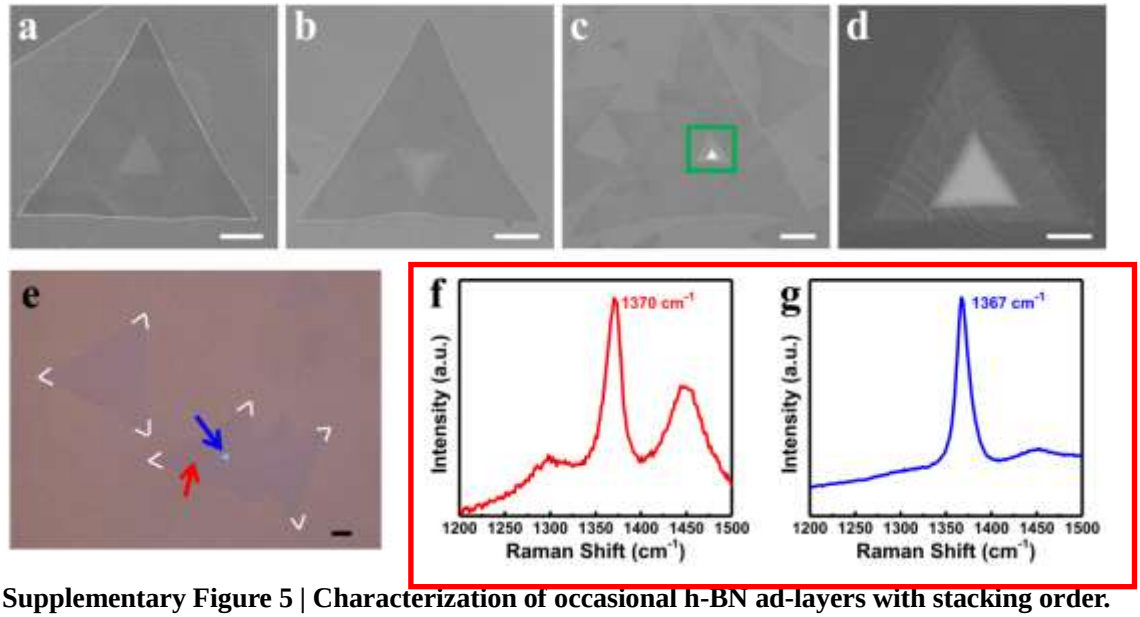

Supplementary Figure 5 | Characterization of occasional h-BN ad-layers with stacking order. (**a-c**) SEM images of h-BN grains with ad-layers. (**d**) Higher magnification of the green square region in (**c**). It can be seen that edges of the ad-layers are parallel or anti-parallel to the first layer, indicating the epitaxial relations between the h-BN multilayers. (**e**) Optical image of h-BN grains on a 90 nm SiO_2/Si substrate with the blue arrow shows the site of the ad-layers. (**f-g**) Raman spectra taken from the areas pointed out by the red and blue arrows in (**e**), respectively. Scale bars: (**a-c,e**) 10 μm, (**d**) 2 μm.

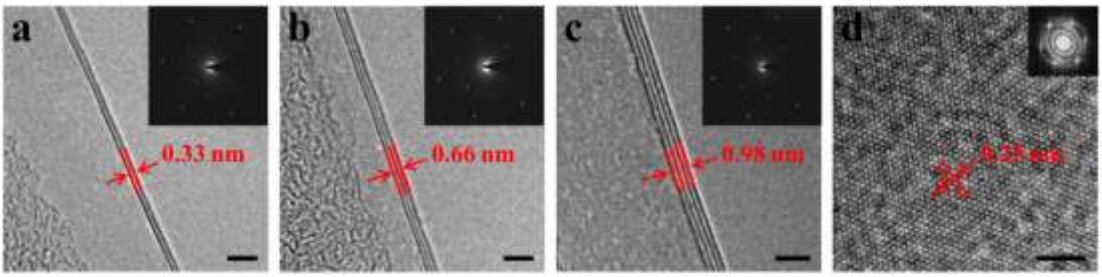

Supplementary Figure 6 | TEM characterization of h-BN films containing more than one layer. (**a-c**) HRTEM images of the folded edges of 2-4 layers h-BN film, respectively. The interlayer distance of h-BN is measured 0.32-0.33 nm. The corresponding SAED pattern presented as the inset in each figure shows a set of characteristic 6-fold symmetric spots, indicating the well-crystalline structure of the h-BN grains. (**d**) HRTEM image of a multilayer h-BN film presenting the hexagonal lattice with a spacing of about 0.25 nm. The inset is the corresponding fast Fourier transform (FFT) pattern. All scale bars are 2 nm.

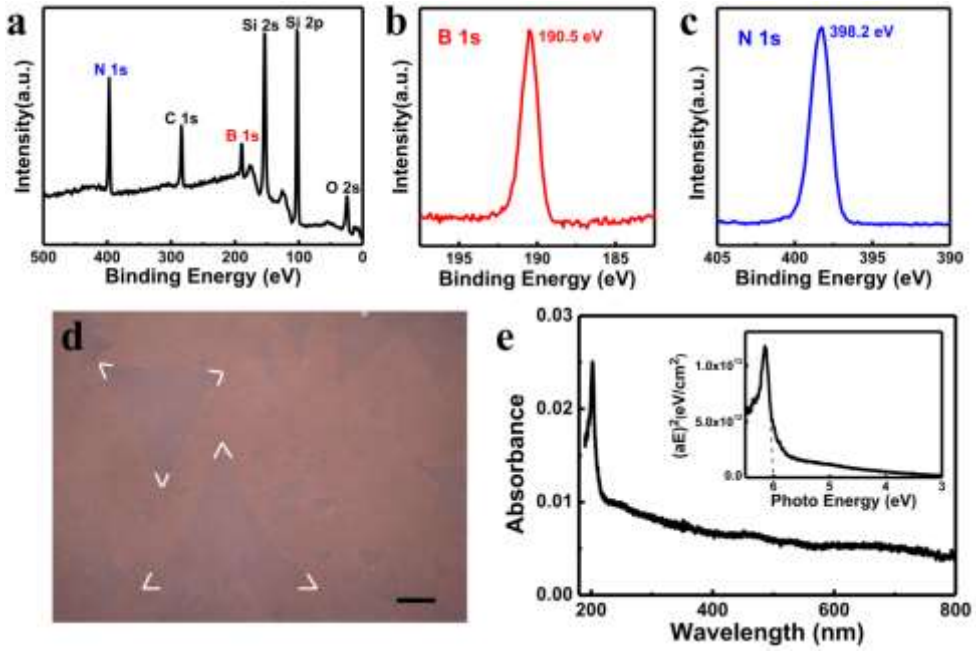

Supplementary Figure 7 | Characterization of h-BN grains transferred onto SiO_2/Si and quartz. (**a**) X-ray photoemission spectroscopy (XPS) spectrum of h-BN on a SiO_2/Si substrate. (**b,c**) The corresponding XPS spectra of B 1s and N 1s showing the peaks located at 190.5 and 398.2 eV, respectively. The B: N atomic ratio calculated is 1.05:1. (**d**) Optical image of h-BN grains on a 90 nm SiO_2/Si substrate. The scale bar is 20 μm. (**e**) Optical absorption spectrum of a monolayer h-BN film displaying an absorbance peak at about 202 nm with an intensity of 2.5 %. The optical bandgap (OBG) is calculated to be about 6.0 eV, as shown in the inset.

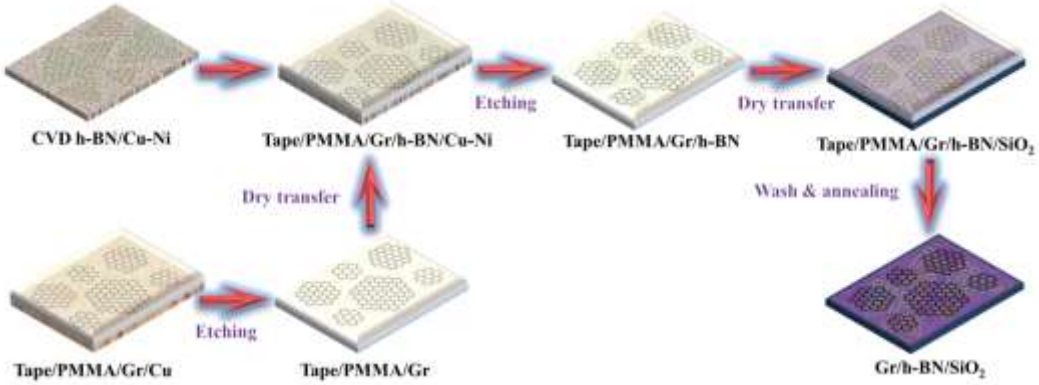

Supplementary Figure 8 | Schematic illustration of the process of transferring graphene and h-BN grains to form graphene/h-BN/SiO_2/Si structure.

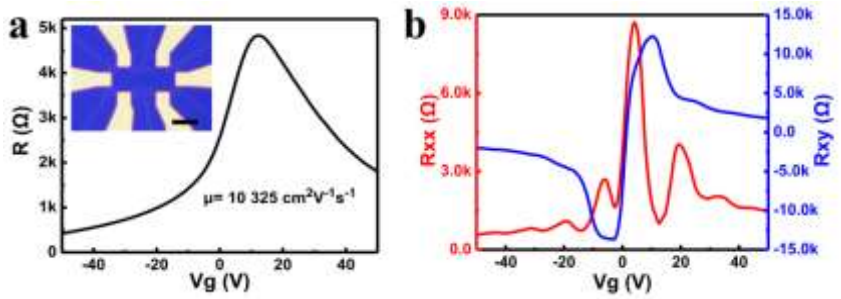

Supplementary Figure 9 | Electronic properties of CVD-grown graphene on transferred CVD-grown multilayer h-BN films. (**a**) Resistivity of the graphene/h-BN Hall bar device versus the back gate voltage at room temperature. The extracted carrier mobility is ~10,325 $cm^2V^{-1}s^{-1}$. The upper inset shows the optical image of the device. (**b**) Graphene/h-BN Hall device exhibits half-integer quantum Hall effect measured at 4 K under a magnetic field B = 9 T. The scale bar in inset in (**a**) is 10 μm.